

High-order harmonic generation and multi-photon ionization of ethylene in laser fields

Z.P. Wang,^{1,2,3} P.M. Dinh,³ P.-G. Reinhard,⁴ E. Suraud³ and F.S. Zhang^{1,2*}

¹*The Key Laboratory of Beam Technology and Material Modification of Ministry of Education, College of Nuclear Science and Technology, Beijing Normal University, Beijing 100875, People's Republic of China*

²*Beijing Radiation Center, Beijing 100875, China*

³*Laboratoire Physique Quantique (IRSAMC), Université P.Sabatier, 118 Route de Narbonne, 31062 Toulouse, cedex, France*

⁴*Institut für Theoretische Physik, Universität Erlangen, Staudtstrasse 7, D-91058 Erlangen, Germany*

(Dated: February 3, 2022)

Applying time-dependent local density approximation (TDLDA), we study the high-order harmonic generation (HHG) of ethylene subjected to the one-color ($\omega = 2.72$ eV) and the two-color ($\omega_1 = 2.72$ eV and $\omega_2 = 5.44$ eV) ultrashort intense laser pulses. The HHG spectrum of ethylene in the one-color laser field shows the obvious plateaus and odd order harmonics are produced while the two-color laser field can result in the breaking of the symmetry and generation of the even order harmonic. The ionization probabilities are obtained showing the increase of the ionization probability of higher charge state by the two-color laser field. The temporal structures of HHG spectrum of ethylene is explored by means of the time-frequency analysis showing new insights of the HHG mechanisms in the one-color and the two-color laser fields.

PACS numbers: 42.65, 33.80, 34.80

I. INTRODUCTION

The interaction between strong laser and atoms and molecules is a hot topic. A series of nonlinear phenomena appear when atoms and molecules are subjected to intense laser pulse [1, 2, 3, 4]. High-order harmonic generation (HHG) is one of the most studied effects among these nonlinear phenomena with the results that the coherent emitted light can be harnessed to produce new coherent trains of extremely short pulses on the time scale of electron motion [5, 6]. A simple model [7], based on the idea of tunnelling ionization of an electron in an atom allows for interpreting the harmonic generation process in terms of recolliding electron trajectories and leads to a universal cutoff law for the maximum in photon energy in harmonic generation. The extra degrees of freedom and nonspherical symmetry of molecules lead to a further new phenomena such as molecular high-order harmonic generation (MHOHG) [5, 6, 8], charge resonance enhanced ionization (CREI) [9, 10] and bond softening [11, 12]. The theoretical understanding of these mechanisms needs to solve the time-dependent Schrödinger equation for all electrons and all nuclear degrees of freedom. However, this kind of numerical solutions only exist for smallest systems, such as atoms [13, 14], H_2 and H_2^+ [16, 17, 18, 19, 29]. For large systems the computation is quite expensive due to the number of degrees of freedom. In contrast, the well tested time dependent Density Functional Theory at the level of the time-dependent local-density approximation (TDLDA) [20] serves as a powerful tool to study the electron dynamics of multi-electron systems [21, 22, 23]. Recently, Madsen *et al*

[24] studied MHOHG of polyatomic molecules using a quantum-mechanical three-step model.

The application of two-color laser field for HHG is a fascinating topic of research science. One can control the formation of harmonic spectrum and yields of ion or molecular fragments by changing the relative phase between the fundamental frequency and its second harmonic fields in the two-color laser field. At present, in experiment and theory, two-color laser field has been applied to atoms [25, 26, 27], molecules [28, 29, 30, 31, 32] and clusters [33, 34, 35]. However, much less has been done for more complicated molecules. In this paper we apply TDLDA, augmented with an average-density self-interaction correction (ADSIC) [36] to investigate theoretically the ionization and MHOHG of ethylene in one-color and two-color laser fields.

II. THEORY

In this section, we represent the real-time method in TDLDA. The molecule is described as a system composed of valence electrons and ions. The interaction between ions and electrons is described by means of a norm-conserving pseudopotentials.

Valence electrons are treated by TDLDA, augmented with an average-density self-interaction correction (ADSIC) [36]. They are represented by single-particle orbitals $\phi_j(\mathbf{r}, t)$ satisfying the time-dependent Kohn-Sham (TDKS) equation [37],

$$\begin{aligned} i\frac{\partial}{\partial t}\phi_j(\mathbf{r}, t) &= \hat{H}_{KS}\phi_j(\mathbf{r}, t) \\ &= \left(-\frac{\nabla^2}{2} + V_{eff}(\mathbf{r}, t)\right)\phi_j(\mathbf{r}, t), \\ j &= 1, \dots, N. \end{aligned} \quad (1)$$

*Corresponding author. Email: fszhang@bnu.edu.cn

V_{eff} is Kohn-Sham effective potential composed of four parts,

$$V_{eff}(\mathbf{r}, t) = V_{ion}(\mathbf{r}, t) + V_{ext}(\mathbf{r}, t) + V_H[n](\mathbf{r}, t) + V_{xc}[n](\mathbf{r}, t), \quad (2)$$

where $V_{ion} = \sum_I V_{ps}(\mathbf{r} - \mathbf{R}_I)$ is ionic background potential, V_{ext} is external potential, V_H stands for a time-dependent Hartree part and the final part is exchange-correlation (xc) potential. The electron density is given by

$$n(\mathbf{r}, t) = \sum_j |\phi_j(\mathbf{r}, t)|^2, \quad (3)$$

and the Hartree potential $V_H[n](\mathbf{r}, t)$ is defined as

$$V_H[n](\mathbf{r}, t) = \int d^3r' \frac{n(\mathbf{r}', t)}{|\mathbf{r} - \mathbf{r}'|}. \quad (4)$$

The xc potential $V_{xc}[n](\mathbf{r}, t)$ is a functional of the time-dependent density and has to be approximated in practice. The simplest choice consists in the TDLDA, defined as

$$V_{xc}^{TDLDA}[n](\mathbf{r}, t) = d\epsilon_{xc}^{hom}(n)/dn|_{n=n(\mathbf{r}, t)}, \quad (5)$$

where $\epsilon_{xc}^{hom}(n)$ is the xc energy density of the homogeneous electron gas. For ϵ_{xc}^{hom} we use the parametrization of Perdew and Zunger [38]. The form of pseudopotential for covalent molecule is taken from [39] including nonlocal part.

The ground state wavefunctions are determined by the damped gradient method [40]. The TDLDA equations are solved numerically by time-splitting technique [41]. For the nonlocal part contained in Hamiltonian, we deal with it in an additional propagator and treated it with a third-order Taylor expansion of the exponential [40]. The absorbing boundary condition is employed to avoid periodic reflecting electrons [42].

For the laser field, neglecting the magnetic field component can be written as

$$E(t) = E_0 f(t) [\cos(\omega(t)) + A \cos(2\omega(t) + \phi)] \quad (6)$$

where $E_0 \propto \sqrt{I}$, I denoting the laser intensity, ω is the laser frequency and $f(t)$ is the pulse profile. A is the electric field strength ration between the two frequency and ϕ is the relative phase. In this paper, A is chosen 0 and 0.5 respectively for the one-color and the two-color laser field and $\phi = 0$.

The laser induced electron dipole moment can be obtained by

$$D(t) = \int r n(\mathbf{r}, t) d^3r \quad (7)$$

The Fourier transform of $D(t)$ gives the MHOHG power spectrum $|D_F(\omega)|^2$.

The harmonics intensity as a function of harmonic frequency ω and emission time β can be obtained by the time-frequency analysis [43]

$$D_G(\omega, \beta) = \left| \int D(t) e^{i\omega t} e^{-(t-\beta)^2/2\alpha^2} dt \right|^2 \quad (8)$$

where the window function width α is chosen as one-tenth of the laser optical period.

The number of escaped electrons is defined as

$$N_{esc} = N_{t=0} - \int_V d^3r n(\mathbf{r}, t) \quad (9)$$

where V is a volume surrounding molecule. A detailed link with experiments is the probabilities $P^k(t)$ of finding the excited molecules in one of the possible charge states k to which they can ionize. The formula can be obtained from [42].

III. RESULTS AND DISCUSSION

The ethylene is the simplest organic π system holding D_{2h} symmetry. In our calculation, there are 12 valence electrons. It is in x - y plane with the center of mass at the origin. The laser polarization is along x direction which is parallel to the axis of CC double bond. The laser time profile is chosen the Ramp envelope. The ramp-on and ramp-off time are both 8 fs and the duration is 30 fs. For the one-color laser field, $I = 10^{14}$ W/cm² and $\omega = 2.72$ eV and for the two-color laser field, $I_1 = 10^{14}$ W/cm², $I_2 = I_1/4$ and $\omega_1 = 2.72$ eV, $\omega_2 = 5.44$ eV. It should be noted that the two-color laser field is non-symmetric, which is the same as that in [31], the negative and positive amplitudes of the electric field strength are not equal.

A. Ionization properties

Fig. 1 shows the time evolutions of the number of escaped electrons of ethylene in the one-color and the two-color laser fields. One can find that the electron emission takes the same pattern in both cases. The ionizations start at around 5 fs with a constant speed in both cases, while it is obvious that electrons start to escape a little earlier in the two-color laser field. Then in both cases electron emissions become more and more slow. Finally, at around 42 fs they are saturated at 1.18 in the two-color case and 0.42 in the one-color case, which is 4 fs earlier than the laser pulses are switched off. Moreover, it is obvious that the ionization is enhanced by the two-color laser field.

Fig. 2 represents ionization probabilities of various charge states for ethylene in one-color and two-color laser fields. From Fig. 2(a) we can see that in the first 5 fs, there is mainly neutral ethylene in the one-color laser field and probabilities of $P^{(1+)}$ and $P^{(2+)}$ are almost zero.

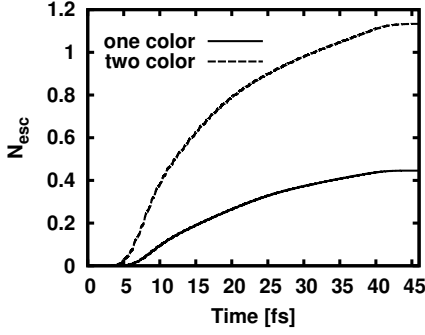


FIG. 1: Time evolutions of the number of escaped electrons of ethylene in the one-color and the two-color laser fields. Solid line: one-color ($\omega = 2.72$ eV) laser field with $I = 10^{14}$ W/cm². Dashed line: two-color laser field with $\omega_1 = 2.72$ eV, $I_1 = 10^{14}$ W/cm² and $\omega_2 = 5.44$ eV, $I_2 = I_1/4$, the relative phase $\phi = 0$.

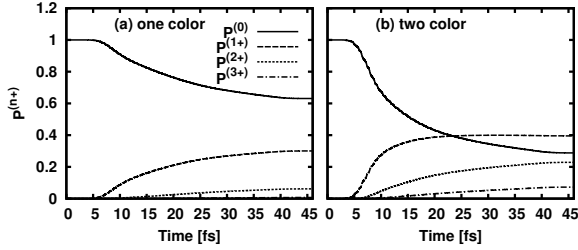


FIG. 2: The ionization probabilities of ethylene in the one-color laser field (a) and two-color laser field (b) for the same cases as in Fig. 1.

Then from 5 fs to 42 fs, the probability of neutral ethylene decreases more and more slowly and reaches a saturated value 0.62 before the laser is switched off. During this period, $P^{(1+)}$ and $P^{(2+)}$ increase more and more slowly and they are also saturated at 42 fs. Their final values are 0.3 and 0.05 respectively. The probability of $P^{(3+)}$ is so small that it is not visible in the figure. Furthermore, one can find that in the course of the one-color laser pulse, neutral ethylene predominates the main probability.

For the ionization probabilities of ethylene in the two-color laser field, as shown in Fig. 2(b), it is obvious that the time evolution pattern is different from that in the one-color case. In the first 5 fs, there is mainly neutral ethylene in the two-color laser field. From 5 fs to 42 fs, $P^{(0)}$ decreases more and more slowly and reaches a saturated value 0.28. This value is smaller than that in Fig. 2(a). It is noteworthy that from 5 fs to 10 fs, $P^{(0)}$ drops quickly from 1 to 0.62 in the two-color case while it takes 37 fs for $P^{(0)}$ to drop from 1 to 0.62 in the one-color case. In Fig. 2(b), $P^{(1+)}$ starts to increase quickly at around 5 fs and it exceeds $P^{(0)}$ at around 23 fs. Finally, it is saturated at 0.4. For $P^{(2+)}$, it starts to

increase at around 7 fs, which is a little later than $P^{(1+)}$, but earlier than $P^{(3+)}$. The increase trends of $P^{(2+)}$ and $P^{(3+)}$ are quite similar. Both of them increase slowly and reach saturated values 0.22 and 0.06 respectively at around 42 fs. We can also find that after 23 fs, $P^{(1+)}$ dominates mainly the charge state.

From the above discussion we can say that the probability of higher charge state is larger for the two-color than that for the one-color laser field. This is related to the fact that the local maximum of amplitude strength for the two-color laser field is larger than for the one-color case. This is consistent with the result from the interaction between atoms and laser fields [44].

B. Analysis of MHOHG

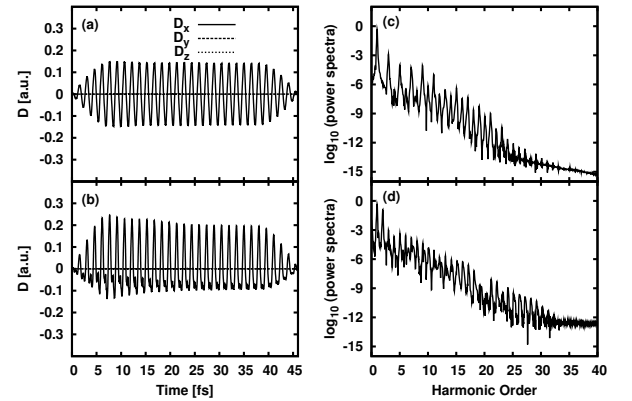


FIG. 3: (a) and (b): the time evolution of dipole moments of ethylene along x , y and z directions in the one-color and the two-color laser fields. (c) and (d): MHOHG spectrum of ethylene in the one-color and two-color laser fields. The laser parameters are the same as those in Fig. 1.

Figs. 3(a) and (b) exhibit the time evolution of dipole moments along x , y and z directions of ethylene in the one-color (ω) and the two-color ($\omega + 2\omega$) laser field respectively. One can find that in both cases the dipole moments along x direction are distinct while those along y and z directions are very small. This is due to the laser polarization is along x direction. However, D_x displays the different behaviors in two cases. In Fig. 3(a), D_x exhibits the relative symmetry while in Fig. 3(b) it is not symmetric because of the non-symmetric property of the electric field strength of the two-color laser field.

The MHOHG spectra calculated by our TDLDA in the one-color and the two-color laser fields are shown in Figs. 3(c) and Fig. 3(d). It is well known that the chosen laser intensities and frequencies are certain essential physical parameters which allow for quasistatic interpretations of strong field laser-atom processes [7, 45]. In this paper, ponderomotive energy $U_p = eI/4m\omega^2$ for $\omega = 2.72$ eV and $2\omega = 5.44$ eV are 1.93 eV and 0.12 eV

respectively. The Keldysh parameter γ separating multiphoton and tunnelling ionization regimes for ethylene ionization potential $I_p = 11.5$ eV is $\gamma = \sqrt{I_p/2U_p} = 1.7$. Thus the present parameters situate our calculations above the tunnelling ionization regime.

According to the atomic HG cut-off law, $E_{max} = I_p + 3.17U_p$, the cutoff MHOHG of ethylene in the one-color laser field is at 6. From the MHOHG spectrum in Fig. 3(c) we can find a clearly cut-off at the 9th order. Although this value is not exactly the same as the value predicted by the atomic HG cut-off law, it is quite near and we attribute the difference to the fact that ethylene is polyatomic molecule while the cut-off law is for atoms. One can also find in Fig. 3(c) that the MHOHG spectrum of ethylene consists of a series of peaks, first decreasing in amplitude and then reaching a plateau. The plateau is rather short from the 5th order harmonic to the 9th order followed by continuously decrease. Thus the MHOHG spectrum of ethylene behaves basically like an atom with recollision of the electron with the compact molecular ion being the principal HG mechanism. Furthermore, one can find in Fig. 3(c) that ethylene generates odd harmonics.

Compare the harmonic spectrum in Fig. 3(d) to that in Fig. 3(c), we can see that the shapes of MHOHG spectrum are different. In Fig. 3(d), the plateau is not so obvious and the decrease lasts longer. This is due to the interference effect of the 1ω and 2ω components of the two-color laser field. It can also be found that even harmonics are well produced in the two-color case. One explanation of this is that even harmonic results from the sum of an odd number of 2ω photon plus two 1ω photons. The other interpretation is that even harmonic generation requires broken reflection symmetry because only this allows that even harmonic generation transforms a squared dipole excitation into one dipole signal, i.e., $\hat{D}^2 \rightarrow \hat{D}$. That transition cannot be mediated by a reflection symmetric system because parity is then conserved, but \hat{D} has negative parity while \hat{D}^2 has positive parity. Ethylene is symmetric and a two-color laser field breaks the symmetry so that a series of even harmonics are produced.

To investigate the detailed temporal structure of the MHOHG spectrum of ethylene, we perform the Gabor transform of the dipole moments in the one-color and the two-color laser field respectively. The laser parameters are the same as those in Fig. 1. Here we consider two typical harmonics which are both in the plateau, one is odd harmonic (5th) and the other one is even harmonic (6th), as shown in Fig. 4. It should be noted that the optical cycle refers to the one-color laser frequency. In Fig. 4(a) we can find that in the one-color laser field, the time profile of the 5th harmonic shows a relative smooth function of the driving laser pulse which indicates that the multiphoton mechanism dominates this lower harmonic regime. However, for the two-color case, the time profile of the 5th harmonic is stronger and it exhibits well the one burst within each optical cycle from the 5th opti-

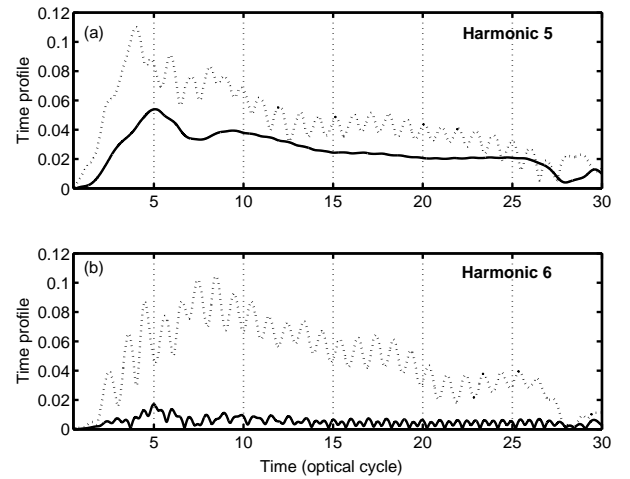


FIG. 4: Time profiles of the harmonics at about the 5th one and the 6th one in the one-color laser field (solid line) and the two-color laser field (dotted line). The laser parameters are the same as those in Fig. 1.

cal cycle to the 25th optical cycle. This can be attributed to the recollision of the electronic wave packet with the ionic cores. Due to the first five and the final five optical cycles are ramp-on and ramp-off times of laser pulses, there are only two and four bursts in these two parts of times. For the 6th harmonic, as shown in Fig. 4(b), it is obvious that in the one-color laser field, the time profile of the 6th harmonic is very weak, whereas in the two-color laser field, it is almost two orders of magnitude stronger. Again, it shows well the one burst within each optical cycle from the 5th optical cycle to the 25th optical cycle.

IV. CONCLUSIONS

In this paper, we have simulated the MHOHG spectra and ionization of ethylene induced by the one-color and the two-color laser fields in the multiphoton regimes with TDLDA. We find that the ionization and the ionization probability of higher charge state are enhanced by the two-color laser field. It is shown that the MHOHG spectrum of ethylene in the one-color laser field exhibits the typical atom HHG spectrum and odd order harmonics are produced. The two-color laser field can result in the breaking of the symmetry and generate the even order harmonics. Furthermore, the detailed temporal structure of MHOHG spectrum of ethylene is obtained by means of the time-frequency transform providing new insights of the MHOHG mechanisms in the one-color and two-color laser fields.

ACKNOWLEDGEMENTS

This work was supported by the National Natural Science Foundation of China (Grants No. 10575012 and No. 10435020), the National Basic Research Program of

China (Grant No. 2006CB806000), the Doctoral Station Foundation of Ministry of Education of China (Grant No. 200800270017), the scholarship program of China Scholarship Council and the French-German exchange program PROCOPE Grant No. 04670PG.

-
- [1] R. J. Levis, G. M. Menkir, and H. Rabitz, *Science* **292**, 709 (2001).
 - [2] K. Yamanouchi, *Science* **295**, 1659 (2002).
 - [3] R. Bartels, S. Backus, E. Zeek, L. Misoguti, G. Vdovin, I. P. Christov, M. M. Murnane, and H. C. Kapteyn, *Nature* (London) **406**, 164 (2000).
 - [4] J. H. Eberly, J. Javanainen, and K. Razzewski, *Phys. Rep.* **204**, 331 (1991).
 - [5] P. B. Corkum and F. Krausz, *Nature Phys.* **3**, 381 (2007).
 - [6] P. Agostini and L. F. DiMauro, *Rep. Prog. Phys.* **67**, 813 (2004).
 - [7] P. B. Corkum, *Phys. Rev. Lett.* **71**, 1994 (1993).
 - [8] J. Itatani, J. Levesque, D. Zeidler, and Hiromichi Nikura, *Nature* (London) **432**, 867 (2004).
 - [9] T. Zou and A. D. Bandrauk, *Phys. Rev. A* **52**, R2511 (1995).
 - [10] T. Seideman, M. Y. Ivanov, and P. B. Corkum, *Phys. Rev. Lett.* **75**, 2819 (1995).
 - [11] G. Yao and S. Chu, *Phys. Rev. A* **48**, 485 (1993).
 - [12] K. Sändig, H. Figger, and T. W. Hänsch, *Phys. Rev. Lett.* **85**, 4876 (2000).
 - [13] J. P. Hansen, J. Lu, L. B. Madsen, and H. M. Nilsen, *Phys. Rev. A* **64**, 033418 (2001).
 - [14] J. S. Parker, L. R. Moore, D. Dundas, and K. T. Taylor, *J. Phys. B* **33**, L691 (2000).
 - [29] S. Chelkowski, T. Zuo, O. Atabek, and A. D. Bandrauk, *Phys. Rev. A* **52**, 2977 (1995).
 - [16] T. Kreibich, M. Lein, V. Engel, and E. K. U. Gross, *Phys. Rev. Lett.* **87**, 103901 (2001).
 - [17] A. D. Bandrauk, S. Chelkowski, S. Kawai, and H. Lu, *Phys. Rev. Lett.* **101**, 153901 (2008).
 - [18] X.-B. Bian, L.-Y. Peng, and T.-Y. Shi, *Phys. Rev. A* **77**, 063215 (2008).
 - [19] L.-Y. Peng, Q.-H. Gong, and A. F. Starace, *Phys. Rev. A* **77**, 065403 (2008).
 - [20] *Density Functional Theory*, NATO ASI, Ser. B (Plenum Press, New York, 1995), Vol. 337.
 - [21] F. Calvayrac, P. G. Reinhard, E. Suraud, and C. A. Ullrich, *Phys. Rep.* **337**, 493 (2000).
 - [22] N. Takashi and K. Yabana, *J. Chem. Phys.* **114**, 2550 (2001).
 - [23] M. Ben-Nun and T. J. Martínez, *Chem. Phys.* **259**, 237 (2000).
 - [24] C. B. Madsen and L. B. Madsen, *Phys. Rev. A* **76**, 043419 (2007).
 - [25] I. J. Kim, C. M. Kin, H. T. Kim, G. H. Lee, J. Y. Park, D. J. Cho, and C. H. Nam, *Phys. Rev. Lett.* **94**, 243902 (2005).
 - [26] D. W. Schumacher and P. H. Bucksbaum, *Phys. Rev. A* **54**, 4271 (1996).
 - [27] J. T. Zhang, S. H. Li, and Z. Z. Xu, *Phys. Rev. A* **69**, 053410 (2004).
 - [28] B. SSheely, B. Walker, and L. F. D. Mauro, *Phys. Rev. Lett.* **74**, 4799 (1995).
 - [29] S. Chelkowski, M. Zamojski, and A. D. Bandrauk, *Phys. Rev. A* **63**, 023409 (2001).
 - [30] K. Haruimiya, H. Kono, Y. Fujimura, L. Kawata, and A. D. Bandrauk, *Phys. Rev. A* **66**, 043403 (2002).
 - [31] X. B. Bian, L. Y. Peng and T. Y. Shi, *Phys. Rev. A* **77**, 063415 (2008).
 - [32] Z. Y. Chen, W. Q. Qu and Z. Z. Xu, *Chin. Phys.* **9**, 577 (2000).
 - [33] H. S. Nguyen, A. D. Bandrauk, and C. A. Ullrich, *Phys. Rev. A* **69**, 063415 (2004).
 - [34] F. S. Zhang, F. Wang, and Y. Abe, *Int. J. Mod. Phys. B* **19**, 2687, (2005).
 - [35] Zhang Y P, Zhang F S, Meng K L and Xiao G Q 2007 *Chin. Phys.* **16** 83
 - [36] Legrand C, Suraud E and Reinhard P G 2002 *J. Phys. B* **35** 1115
 - [37] Gross E K U and Kohn W 1990 *Adv. Quant. Chem.* **21** 255
 - [38] Perdew J P and Zunger A 1981 *Phys. Rev. B* **23** 5048
 - [39] Goedecker S, Teter M and Hutter J 1996 *Phys. Rev. B* **54** 1703
 - [40] Calvayrac F 1998 *Ann. Phys. (Paris)* **23** 1
 - [41] Calvayrac F, Reinhard P G and Suraud E 1997 *Ann. Phys. (NY)* **255** 125
 - [42] Ullrich C A 2000 *J. Mol. Struct. (THEOCHEM)* **501-502** 315
 - [43] Antoine P, Piraux B and A. Maquet 1995 *Phys. Rev. A* **51** R1750
 - [44] Tong X M and Chu S I 2001 *Phys. Rev. A* **64** 013417
 - [45] Scrinzi A, Geissler M and Brabec T 1999 *Phys. Rev. Lett.* **83** 706